

# Cotransport of clay colloids and viruses through both horizontal and vertical water-saturated columns: Downward and Upward flows

V.I. Syngouna<sup>1\*</sup> and C.V. Chrysikopoulos<sup>2</sup>,

<sup>1</sup>Environmental Engineering Laboratory, Department of Civil Engineering, University of Patras, 26500 Patras, Greece

<sup>2</sup>Department of Environmental Engineering, Technical University of Crete, 73100 Chania, Greece

\*Corresponding author: E-mail: vsyngouna@upatras.gr, Tel +30 2610996530

## Abstract

The cotransport of clay colloids and viruses in laboratory packed columns, in both horizontal (H) and vertical (V) orientations, was investigated. Bacteriophages MS2 and  $\Phi$ X174 were used as model viruses, kaolinite (KGa-1b) and montmorillonite (STx-1b) as model clay colloids. A steady flow rate of  $Q=1.5$  mL/min was applied in horizontal, vertical upward (VU) and downward (VD) directions. For the most cases examined, estimated mass recovery values were higher in VD than VU flows suggesting that flow direction has a significant influence on the particle deposition. For all transport experiments, slight enhancement was observed for both viruses and clay colloids except the case of the VU and VD flows of  $\Phi$ X174 and STx-1b. Mass recovery values for both viruses, calculated based on total virus concentration in the effluent, were reduced compared to those in the absence of clays. In the presence of KGa-1b, at H and VD flow directions, clay colloids hindered the transport of  $\Phi$ X174 while in the presence of STx-1b at all flows (H,VU,VD), the presence of clay colloids facilitated the transport of  $\Phi$ X174. Moreover, both clays hinder MS2 in all cases examined except VU and VD flow directions in the presence of STx-1b.

*Keywords: viruses,  $\Phi$ X174, MS2, clay minerals, KGa-1b, STx-1b, cotransport, flow direction*

## 1. INTRODUCTION

Numerous experimental and theoretical studies have focused on factors that govern colloid and biocolloid (e.g. viruses, bacteria) transport in fractured and porous media [1, 2, 3, 4, 5, 6, 7]. In the recent years numerous investigators have examined theoretically and experimentally the role of velocity on colloid transport and deposition in addition to the influence of either the particle size [1, 5] or ionic strength [8]. Other factors that have been evaluated include the role of roughness and flow direction [9], porous media collector size [5], and pore geometry or grain angularity [10]. Moreover, the presence of colloids suspended in the aqueous phase has been shown either to enhance or hinder the transport of organic and inorganic pollutants [11, 12, 13]. However, the effect of flow direction on colloid and biocolloid transport in porous media has received relatively minor attention [14]. Flow direction in the experimental investigations are either horizontal [5, 13, 15] downward [2, 3] or upward in order to minimize air entrapment [1]. Previous experimental observations show that flow direction can have a significant influence on colloid deposition. Thus, understanding the influence of flow direction on the cotransport of clay colloids and viruses is of practical significance.

The present study examines the effect of flow direction on the cotransport of clay colloids and viruses in horizontal and vertical water-saturated columns packed with glass beads. Bench scale experiments were performed to investigate the interactions between viruses and clays during their simultaneous transport (cotransport) in porous media. Also the synergistic effects of suspended clay colloids and flow direction on the attenuation and transport of viruses in porous media is examined.

## 2. MATERIALS AND METHODS

### 2.1. Bacteriophages and assay

The bacteriophage MS2 (F-specific single-stranded RNA phage with effective particle diameter ranging from 24 to 26 nm) has been recommended as a surrogate for poliovirus due to similarities in size, and has been employed as a conservative tracer for enteric virus transport, because MS2 sorption onto the majority of soil types is low compared to many other viruses. The bacteriophage  $\Phi$ X174 (somatic single-stranded DNA phage with effective particle diameter ranging from 25 to 27 nm) has been recommended as a surrogate for norovirus due to similarities in size. Both bacteriophages are infecting *E. coli*, and were assayed by the double-layer overlay method, as outlined by Syngouna and Chrysikopoulos [4,5]. For the separation of viruses adsorbed onto clay colloids from suspended viruses in the liquid phase, 0.3 mL of the density gradient separation reagent Histodenz (60% by weight, Axis-Shield PoC AS Company, Norway) was added to 2 mL of the liquid sample [15], the mixture was centrifuged at 2000xg for 30 min so that the supernatant was free of clay colloids. The suspension of unattached viruses in the supernatant was pipetted out and the suspended viruses were determined.

### 2.2. Clays

The clays used in this study were kaolinite (KGa-1b, well-crystallized kaolin, from Washington County, Georgia), and montmorillonite (STx-1b, Ca-rich montmorillonite, Gonzales County, Texas), purchased from the Clay Minerals Society (Columbia, USA). The  $<2 \mu\text{m}$  colloidal fraction, used in transport experiments, was separated by sedimentation and was purified following the procedure described by Rong et al. [16]. The hydrodynamic diameter of the clay colloids was measured by a zetasizer (Nano ZS90, Malvern Instruments) and was found to be equal to  $d_p=842.85\pm 125.85$  nm for KGa-1b, and  $d_p=1187\pm 380.81$  nm for STx-1b. The optical density of the clay colloids was analyzed at a wavelength of 280 nm by a UV-vis spectrophotometer, and the corresponding clay concentrations were determined by the procedures developed by Chrysikopoulos and Syngouna [7].

### 2.3. Column Experiments

Using KGa-1b and STx-1b as the model clay colloids and MS2 and  $\Phi$ X174 bacteriophages as model viruses, we carried out flow through experiments using a 30 cm long Chromaflex glass column packed with 2 mm in diameter glass beads (Fisher Scientific, New Jersey) under specific experimental conditions. Constant flow of sterile ddH<sub>2</sub>O at flow rate of  $q = 1.5$  ml/min, corresponding to pore water velocity of  $U = q/\theta = 0.74$  cm/min, was maintained through the packed column with a peristaltic pump. Note that the columns were placed horizontally ( $\beta=0^\circ$ ) and vertically ( $\beta=\pm 90^\circ$ ). A fresh column was packed for each experiment. One set of flow through experiments was performed with viruses and clay colloids alone in order to determine their individual transport characteristics and another set of cotransport experiments was performed to investigate the simultaneous effect of gravity and clay colloid presence on virus transport in horizontal ( $\beta=0^\circ$ ) and vertical ( $\beta=\pm 90^\circ$ ) columns. For both sets, 3 PV of colloid suspension was injected into the packed column, followed by 3 PV of ddH<sub>2</sub>O. All experiments were carried out at room temperature ( $\sim 25^\circ$  C).

## 3. THEORETICAL CONSIDERATIONS

### 3.1 Moment analysis

The concentration breakthrough data obtained at location  $x=L$  were analyzed by the normalized temporal moments are defined as ([17]):

$$M_n(x) = \frac{m_n(x)}{m_0(x)} = \frac{\int_0^\infty t^n C_i(x,t) dt}{\int_0^\infty C_i(x,t) dt} \quad (1)$$

The first normalized temporal moment,  $M_1$ , characterizes the center of mass of the concentration breakthrough curve and defines the mean breakthrough time or average velocity. Worthy to note is that the ratio  $M_{1(i)}/M_{1(t)}$  indicates the degree of velocity enhancement of colloid particle  $i$  relative to the conservative tracer. If this ratio is less than one, there exists colloid retardation, and if it is greater than one there exists velocity enhancement of colloid transport.

### 3.2. CFT consideration

Classical colloid filtration theory (CFT) was used to quantitatively compare the attachment of viruses onto glass beads and clay colloids. The dimensionless collision efficiency,  $\alpha$  (the ratio of the collisions resulting in attachment to the total number of collisions between suspended particles and collector grains), was calculated from each breakthrough curve [18]. Using the concept of apparent collision efficiency introduced by Walshe et al. [12] two different apparent collision efficiencies were calculated. The first collision efficiency,  $\alpha_{\text{Total-v}}$ , is based on  $C_{\text{Total-v}}$  in the effluent and represents the attachment of  $C_v$  onto both glass beads and  $C_{c^*}$ . The second collision efficiency,  $\alpha_v$ , is based on  $C_v$  in the effluent and represents the attachment of both  $C_v$  and  $C_{vc}$ , onto glass beads, denoted as  $C_{v^*}$  and  $C_{vc^*}$ , respectively, as well as the attachment of  $C_v$  onto both  $C_c$  and  $C_{c^*}$ , denoted as  $C_{vc}$  and  $C_{vc^*}$ .

## 4. RESULTS AND DISCUSSION

### 4.1. Transport experiments

The normalized virus (MS2 and  $\Phi$ X174) and clay colloid (KGa-1b, STx-1b) breakthrough data for the three directional flow conditions (H, VD, VU), are presented in Figure 1.

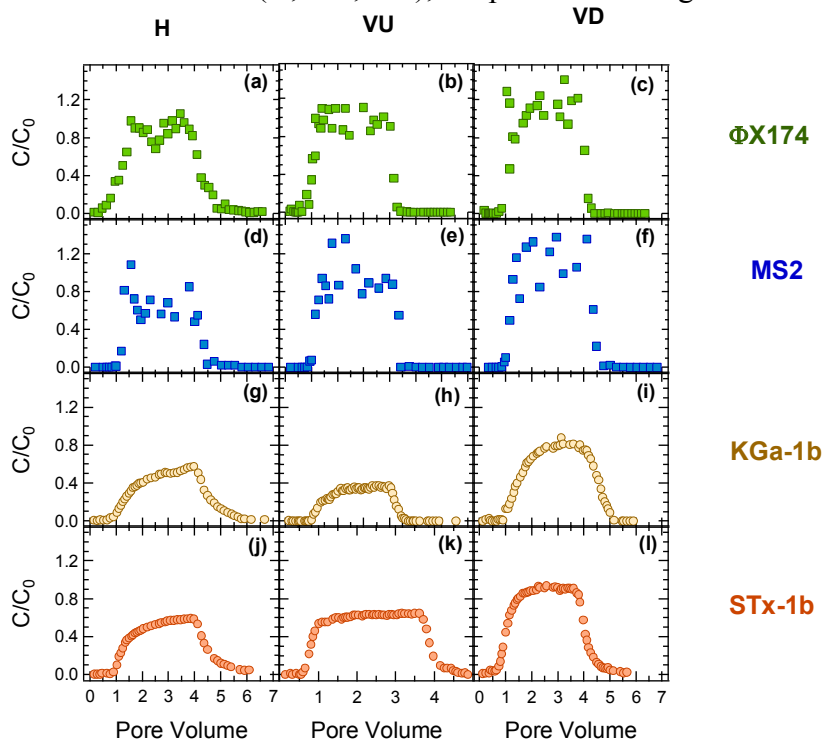
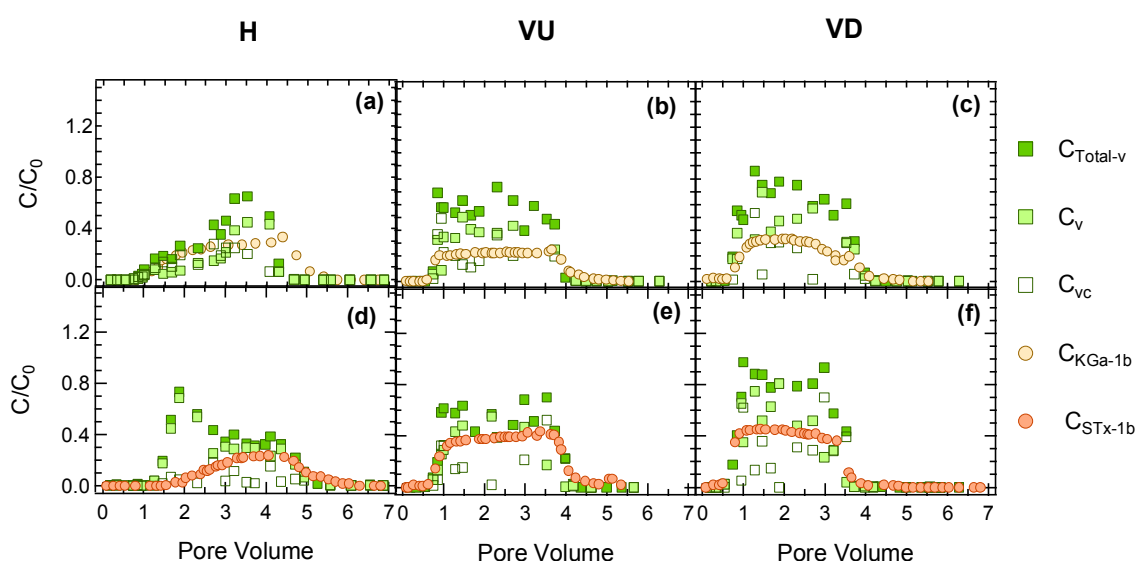


**Figure 1.** Experimental data of viruses (a-c:  $\Phi$ X174 and d-f: MS2) (rectangulars) and clay colloids (g-i: KGa-1b and j-l: STx-1b) (circles) breakthrough in columns packed with glass beads with (a,d,g,i) H-horizontal, (b,e,h,k) VU-vertical upward and (c,f,i,l) VD-vertical downward, directional flow conditions.

With no exception, all estimated  $M_r$  values for MS2 were lower than those of  $\Phi$ X174. Although low  $M_r$  values cannot lead to the conclusion that MS2 particles retained were irreversibly attached or inactivated, the possibility that low  $M_r$  values are caused by irreversible attachment and inactivation cannot be excluded. Consequently, the observed low  $M_r$  values of MS2 may be attributed to the higher attachment and inactivation rates found for MS2 than  $\Phi$ X174. For the most cases examined, slight enhancement was observed for both viruses and clay colloids, while only for the vertical flows of  $\Phi$ X174 and STx-1b the transport of  $\Phi$ X174 was retarded by 2-3% compared to the tracer, and the transport of STx-1b was retarded by 11%. Higher  $M_r$  values were observed for STx-1b than KGa-1b for all cases examined.

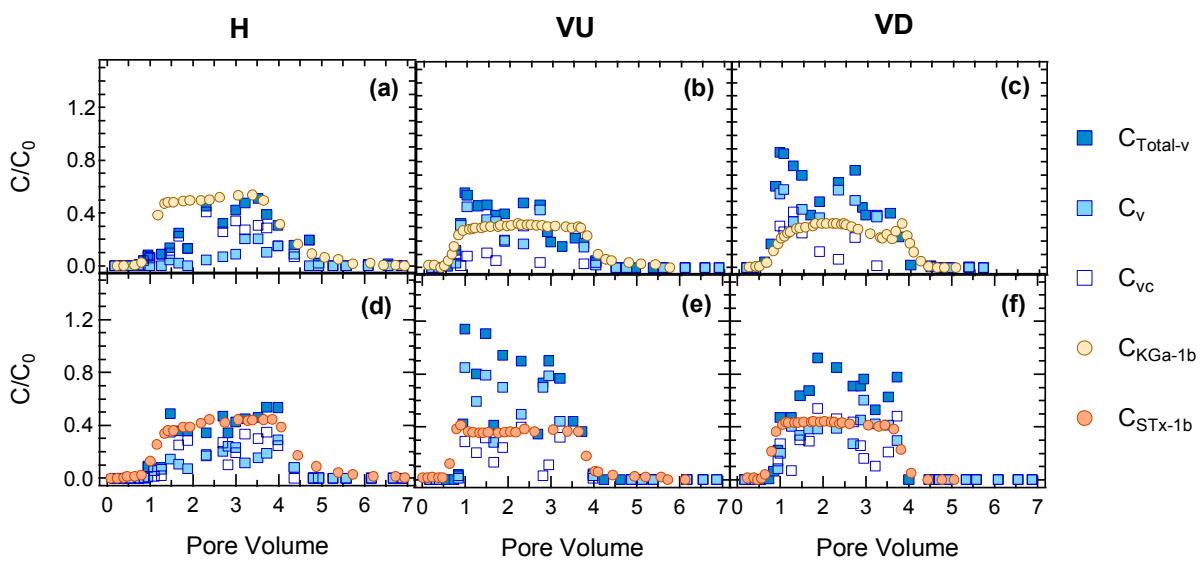
## 4.2. Cotransport experiments

Figure 2 presents the normalized  $\Phi$ X174 and clay (a,c,e: KGa-1b, b,d,f: STx-1b) cotransport breakthrough data for the three directional flow conditions (H, VD, VU). The suspended virus breakthrough concentrations are labelled as  $C_v$ , the total virus concentrations (suspended plus sorbed onto clays) are labelled as  $C_{Total-v} = C_v + C_{vc}$ . The suspended clay breakthrough concentrations are labelled as  $C_c$ , and the concentrations of viruses attached onto suspended clay colloids are labelled as  $C_{vc}$ . The corresponding  $M_r$  values, based on  $C_{Total-v}$  of  $\Phi$ X174 in the effluent, were considerably reduced in the presence of clay colloids compared to those obtained in the absence of them. This suggested that some clay-bound viruses were retained in the column due to clay attachment onto glass beads [15]. Furthermore, the transport of  $C_{Total-v}$  for  $\Phi$ X174 was enhanced (10–14%) only at the horizontal flow direction compared to the tracer, and also KGa-1b and STx-1b were enhanced 20% and 57% only at the horizontal flow condition H, for  $\Phi$ X174 and KGa-1b cotransport. Moreover, the transport of  $C_v$  was enhanced 7% in the presence of KGa-1b, and 22% in the presence of STx-1b compared to the tracer only at the horizontal flow direction H. The same trend was observed for  $C_{vc}$  of  $\Phi$ X174, except when KGa-1b was present at vertical flow conditions (VU,VD), where retardation for  $C_{vc}$  of  $\Phi$ X174 was observed. Note that in the presence of KGa-1b, at H and VD directional flow conditions, clay colloids hindered the transport of  $\Phi$ X174 ( $M_{1(i)}/M_{1(t)}$  of  $C_{Total-v}$ ,  $C_v > M_{1(i)}/M_{1(t)}$  of  $C_{vc} > 1$  or  $M_{1(i)}/M_{1(t)}$  of  $C_{vc} < M_{1(i)}/M_{1(t)}$  of  $C_{Total-v}$ ,  $C_v < 1$ ). In the presence of STx-1b at all cases examined (H,VU,VD flow directions), the presence of clay colloids facilitated the transport of  $\Phi$ X174 ( $M_{1(i)}/M_{1(t)}$  of  $C_{Total-v}$ ,  $C_v < M_{1(i)}/M_{1(t)}$  of  $C_{vc} < 1$  or  $M_{1(i)}/M_{1(t)}$  of  $C_{vc} > M_{1(i)}/M_{1(t)}$  of  $C_{Total-v}$ ,  $C_v > 1$ ).



**Figure 2.** Experimental data of  $\Phi$ X174 and clay colloids (a-c: kGa-1b, d-f: STx-1b) co-transport in columns packed with glass beads with (a,d) H-horizontal, (b,e) VU-vertical upward and (c,f) VD-vertical downward, directional flow conditions.

Figure 3 presents the normalized MS2 and clay (a,c,e: KGa-1b, b,d,f: STx-1b) cotransport breakthrough data for the three directional flow conditions (H, VD, VU). The various  $M_{1(i)}/M_{1(t)}$  indicated that  $C_{Total-v}$  of MS2 was enhanced (8–14%) compared to the tracer only at the horizontal flow direction compared to the tracer. The same trend was observed at H flow direction for  $M_{1(i)}/M_{1(t)}$  ratios based on  $C_v$  and  $C_{vc}$  of MS2. Also, KGa-1b was enhanced 3% and STx-1b 10% compared to the tracer at H flow condition. At the H direction, all concentrations ( $C_{Total-v}$ ,  $C_v$ ,  $C_{vc}$ , and  $C_c$ ) were significantly enhanced compared to the tracer. Worthy to note is that for all cases examined,  $C_v$  of MS2 was enhanced more than  $C_{Total-v}$  of MS2, and  $C_{Total-v}$  of MS2 was enhanced more than  $C_{vc}$  of MS2 compared to the tracer for both clays employed (KGa-1b, STx-1b). Note that both clays hinder MS2 transport ( $M_{1(i)}/M_{1(t)}$  of  $C_{Total-v}$ ,  $C_v > M_{1(i)}/M_{1(t)}$  of  $C_{vc} > 1$  or  $M_{1(i)}/M_{1(t)}$  of  $C_{vc} < M_{1(i)}/M_{1(t)}$  of  $C_{Total-v}$ ,  $C_v < 1$ ) in all cases examined except vertical flow conditions in the presence of STx-1b ( $M_{1(i)}/M_{1(t)}$  of  $C_{Total-v}$ ,  $C_v < M_{1(i)}/M_{1(t)}$  of  $C_{vc} < 1$ ). Therefore, depending on the physicochemical conditions, colloid particles can facilitate or hinder the transport of viruses in porous media.



**Figure 3.** Experimental data of MS2 and clay colloids (a-c: kGa-1b, d-f: STx-1b) co-transport in columns packed with glass beads with (a,d) H-horizontal, (b,e) VU-vertical upward and (c,f) VD-vertical downward, directional flow conditions.

The  $\alpha_{Total-v}$  values of MS2 in the transport experiments were found to be higher than those of  $\Phi X174$  for all flow directions. This was attributed to the more conservative adsorption behavior of  $\Phi X174$  than that of MS2, which is in agreement with previous results [5]. Moreover, in the presence of clay colloids (cotransport experiments),  $\alpha_{Total-v}$  values were higher for both viruses in all cases examined, which indicated that more attachment sites were available on the solid matrix (glass beads and  $C_c^*$ ). In the presence of both KGa-1b and STx-1b,  $\alpha_{Total-v}$  values were higher in vertical than horizontal flow conditions and higher in upward than downward flows with the only exception of MS2 and STx-1b cotransport. Furthermore, the relative high  $\alpha_v$  values ( $\alpha_v > \alpha_{Total-v}$ ) indicated that the presence of clay colloids increased the attachment of virus onto glass beads and clay colloids. In all cases examined,  $\alpha_v$  values were higher in horizontal than vertical flow conditions. Moreover, the higher  $\alpha_v$  values observed for MS2 in the presence of both KGa-1b and STx-1b could be attributed to the greater affinity of MS2 for both clay particles [7].

### Acknowledgments

This research has been co-financed by the European Union (European Social Fund-ESF) and Greek National Funds through the Operational program “Education and Lifelong Learning” under the action Aristeia I (Code No. 1185). This work is a collaboration between members of the BioMet Network.

## References

1. Keller, A. A., Sirivithayapakorn, S. S., Chrysikopoulos, C.V. (2004). Early breakthrough of colloids and bacteriophage MS2 in a water-saturated sand column, *Water Resour. Res.*, **40**, W08304, doi:10.1029/2003WR002676.
2. Anders, R., and Chrysikopoulos, C.V. (2006). Evaluation of the factors controlling the time-dependent inactivation rate coefficients of bacteriophage MS2 and PRD1, *Environ. Sci. Technol.*, **40(10)**, 3237-3242, doi:10.1021/es051604b.
3. Anders, R., and Chrysikopoulos, C.V. (2009). Transport of viruses through saturated and unsaturated columns packed with sand, *Transp. Porous Media*, **76**, 121–138, doi:10.1007/s11242-008-9239-3.
4. Syngouna, V. I., and Chrysikopoulos, C. V. (2010) Interaction Between Viruses and Clays in Static and Dynamic Batch Systems. *Environ. Sci. Technol.* **44**, 4539–4544.
5. Syngouna, V. I., and Chrysikopoulos, C. V. (2011) Transport of biocolloids in water saturated columns packed with sand: Effect of grain size and pore water velocity. *J. Contam. Hydrol.* **126**, 301-314.
6. Shen, C., Lazouskaya, V., Zhang, H., Wang, F., Li, B., Jin, Y. and Huang, Y. (2012). Theoretical and experimental investigation of detachment of colloids from rough collector surfaces, *Colloids Surf. A*, **410**, 98–110.
7. Chrysikopoulos, C.V., and Syngouna, V.I. (2012) Attachment of bacteriophages MS2 and  $\Phi$ X174 onto kaolinite and montmorillonite: extended DLVO interactions. *Colloids Surf. B: Biointerfaces*. 9274-9283.
8. Tong, M., Ma, H. and Johnson, W.P. (2008). Funneling of flow into grain-to-grain contacts drives colloid-colloid aggregation in the presence of an energy barrier, *Environ. Sci. Technol.*, **42**, 2826–2832.
9. Yoon, J.K., Germaine, J.T. and Culligan, P.J. (2006). Visualization of particle behavior within a porous medium: mechanisms for particle filtration and retardation during downward transport, *Water Resour. Res.*, **42**, W06417, doi:10.1029/2004WR003660
10. Tong, M., and Johnson, W.P. (2006). Excess colloid retention in porous media as a function of colloid size, fluid velocity, and grain angularity, *Environ. Sci. Technol.*, **40**, 7725–7731.
11. Kretzschmar, R., Borkovec, M., Grolimund, D. and Elimelech, M. (1999). Mobile subsurface colloids and their role in contaminant transport. *Adv. Agron.* **66**, 121–194.
12. Walshe, G. E., Pang, L. , Flury, M., Close, M. E., Flintoft, M. (2010). Effects of pH, ionic strength, dissolved organic matter, and flow rate on the cotransport of MS2 bacteriophages with kaolinite in gravel aquifer media, *Water Res.*, **44**, 1255-1269
13. Syngouna, V.I., and Chrysikopoulos, C.V. (2013). Cotransport of clay colloids and viruses in water saturated porous media, *Colloids Surf. A: Physicochem. Eng. Aspects*, **416**, 56–65.
14. Ma, H., Pedel, J., Fife, P., and Johnson, W.P. (2009). Hemispheres-in-cell geometry to predict colloid deposition in porous media, *Environ. Sci. Technol.*, **43**, 8573–8579.
15. Vasiliadou, I. A., and Chrysikopoulos, C. V. (2011). Cotransport of *Pseudomonas putida* and kaolinite particles through water saturated porous media. *Water Resour. Res.*, **47**, W02543 doi:10.1029/ 2010WR009560.
16. Rong, X., Huanga, Q., He, X., Chen, H., Cai, P., and Liang, W. (2008). Interaction of *Pseudomonas putida* with kaolinite and montmorillonite: A combination study by equilibrium adsorption, ITC, SEM and FTIR. *Colloids Surf. B: Biointerfaces*, **64**, 49–55.
17. James, S.C., and Chrysikopoulos, C.V. (2011). Monodisperse and polydisperse colloid transport in water-saturated fractures with various orientations: Gravity effects. *Adv. Water Resour.*, **34**, 1249–1255, doi: 10.1016/j.advwatres.2011.06.001.
18. Rajagopalan, R., and Tien, C.(1976). Trajectory analysis of deep-bed filtration with the sphere-in-cell porous media model. *AIChE J.* **22**, 523-533.
19. Tufenkji, N. and Elimelech, M. (2004). Correlation equation for predicting single-collector efficiency in physicochemical filtration in saturated porous media. *Environ. Sci. Technol.* **38**, 529-536.

# Leaching tests for the estimation and simulation of the transport of TiO<sub>2</sub> nanoparticles through landfill and natural soils

E. Tassi<sup>\*1</sup>, R. Pini<sup>1</sup>, M. Barbafieri<sup>1</sup>, I. Valadao<sup>2</sup> and J.A. de Castro<sup>2</sup>

<sup>1</sup>Institute of Ecosystem Studies, National Research Council, 56124 Pisa, Italy

<sup>2</sup>School of Metallurgical Industrial Engineering, Fluminense Federal University, 27255 Volta Redonda (Rio de Janeiro), Brasil

\*Corresponding author: E-mail: eliana.tassi@ise.cnr.it, Tel +39 050 3152478

## Abstract

The increased use and production of nanomaterials lead to enhance the presence of nanoproducts and nanowastes in the environment. A growing concern regarding the spread of nanostructures in soil and waters and its effects on the environment and human health is coming into light in the recent years. In the present study, we compare and estimate experimentally and mathematically (using the MPHMTM simulation model) the transport and behavior of commercial TiO<sub>2</sub> nanoparticles in two different soils: a soil from a waste-landfill and a natural organic soil. After characterization of collected soil samples, the transport and mobility of aqueous suspensions of TiO<sub>2</sub> nanoparticles were evaluated through columns leaching experiments. Breakthrough curves for both soils were interpreted and the obtained data were used for simulation of nanoparticles' transport. A relative elevated mobility of nanoparticles in the natural organic soil was found: a continuous leaching of about 30% of the inflow Ti concentration. On the other hand, the landfill sandy soil was safer in terms of nanoparticles' mobility, due to its retention on the soil solid phase. Differences in TiO<sub>2</sub> nanoparticles transport could be attributed to different chemistry of soil pore water affecting in different ways their mobility: in the natural organic soil (higher dissolved organic carbon and lower ionic strength) the effective coating of TiO<sub>2</sub> nanoparticles by soluble organic molecules produce an energy barrier between nanoparticles, reducing the size of aggregates and hindering soil adsorption or straining. In landfill sandy soil (high ionic strength) the transport was reduced with nanoparticles collapsing in soil pores by the compression of the electrostatic double layer and with the involvement of the movement of small soil colloids.

*Keywords: TiO<sub>2</sub> NPs, soil properties, transport, column leaching, transport simulation*

## 1. INTRODUCTION

The market of nanotechnology products is growing at enormous speed and it doubles every three years as a result of successive introduction of new materials [1]. The global production of nanoparticles (NPs) was expected to be over 10 million tons, where TiO<sub>2</sub> NPs production reaches 2 million tons per year [2].

At nanosize range (below 100 nm), the properties of materials differ substantially from bulk materials of the same composition, mostly due to the increased specific surface area and reactivity, which may lead to increased bioavailability and toxicity.

Considering the increasing use of nanomaterials and nanoproducts, the presence of NPs in the environment can significantly increase as well as its interaction with the biotic and abiotic component of ecosystems. NPs could be spread in water and soil through several routes [3]: *i*) atmospheric deposition of combustion exhausts; *ii*) land-applied biosolids from conventional waste water treatment plants; *iii*) nanowaste deposition and decomposition on landfill soil [4]; *iv*) through its use in agriculture in several plant protection products and fertilizers [5]; *v*) spill or accident during NPs production or transport. Moreover, beyond the concern about its effects on the